Electronic Excitation Transfer in the LH2 Complex of *Rhodobacter sphaeroides*

Ralph Jimenez, Srivatsan N. Dikshit, Stephen E. Bradforth, and Graham R. Fleming*

Department of Chemistry and the James Franck Institute, University of Chicago, Chicago, Illinois 60637

Received: October 17, 1995; In Final Form: January 17, 1996[⊗]

Ultrafast fluorescence upconversion measurements were carried out on the peripheral (LH2) light harvesting antenna complex of *Rhodobacter sphaeroides* isolated in the detergents *N*-octyl-β-D-glucopyranoside and lauryl dimethylamine oxide. The B800 and B850 bands were excited in separate experiments, and the B850 emission was detected in each case. We make use of the recently determined crystal structure of a purple bacterial LH2 complex to simulate our data and to calculate the exciton level structure of the B850 aggregate. The B800 to B850 excitation transfer occurs with a 650 fs time constant. The depolarization of B850 emission follows a wavelength dependent, biexponential decay with time constants 50−90 and 400−500 fs. We can reproduce the non-exponentiality of the depolarization by assuming incoherent hopping between dimeric sites with a 250 cm^{-1} full width at half-maximum (fwhm) Gaussian distribution of site energies (inhomogeneity). We calculate the homogeneous hopping time between dimers in B850 to be ∼100 fs. The exciton calculations including pigment energetic disorder demonstrate the validity of a hopping picture of excitation transfer within the B850 band at room temperature.

I. Introduction

The initial steps of photosynthesis involve the transfer of absorbed light energy to the photochemical reaction center, where the energy is fixed as an electrochemical gradient.[1] In purple photosynthetic bacteria, light is absorbed and rapidly transported by two types of transmembrane pigment−protein assemblies, the LH2 (peripheral) and LH1 (core) light harvesting complexes. Recently, a high-resolution crystal structure of LH2 has been obtained for *Rps. acidophila*, this along with lower resolution structural information for LH1 has indicated that the bacterial antenna form highly symmetric ringlike structures.[2−4] The high-resolution structure is of great significance because the amino acid sequences and spectroscopic properties of all purple bacterial LH2 complexes (and LH1 complexes) show many similarities. This newly available structural information makes these complexes particularly suited for time resolved spectroscopic studies because they provide models in which experimentally observed time scales may be visualized as the flow of energy among the pigments.

In this work, we make use of subpicosecond fluorescence measurements to resolve the migration of energy within isolated LH2 complexes of *Rhodobacter sphaeroides* (*Rb. sphaeroides*) at room temperature. Unlike LH1, which contains only one near-IR absorption band at 870 nm, the LH2 complexes contain two types of bacteriochlorophyll *a* (BChl*a*), distinguished by their binding sites (and absorption wavelengths) as B800 and B850. These complexes also contain the carotenoid spheroidene. Here, we focus on resolving the time scale of energy transfer between and among the B800 and B850 pigments and comment on the implications of these time scales for the mechanisms of energy transfer.

The high-resolution crystal structure of the peripheral (LH2) complex from *Rps. acidophila* shows a beautiful entanglement of α-helices, each of which coordinates the bacteriochlorophyll pigments into an overall circular structure.[2] The 18 B850s form a ring perpendicular to the membrane plane. The BChl*a* are not quite evenly spaced; the closest distance between BChl*a* rings bound to the same $\alpha\beta$ polypeptide unit is 3.4−3.5 Å, whereas the distance between BChl*a* on neighboring units is 3.8−3.9 Å.[5] The chlorin rings of the BChl*a* appear curved as a result of interactions with the protein; this ring distortion may be responsible for some of the blue shift of B850 compared to LH1. Mutations of amino acids near the binding site of B850 shift its absorption band to the blue as a result of electronic and/or steric interactions.[6,7] The nine B800s are held parallel to the membrane plane, 17.6 Å below the B850s. The center to center distance between B800s is 22 Å, and the Q_y dipoles are arranged with a small tilt from the tangent to the ring. The large separation between the B800s makes it likely that they should be regarded as monomeric BChl*a*, whereas the B850s are arranged such that it may be necessary to consider them as a strongly coupled aggregate.

The energy transfer processes within the LH2 complex have been studied for many years using both steady state and time resolved absorption and emission spectroscopies.[8−19] Studies have been conducted at both low temperatures and room temperature. Optical excitation of the B800 pigments results in energy transfer to B850 in less than 1 ps at room temperature.[9] At temperatures from 4 to 77 K, the excitation transfer is nearly temperature independent and slows down to 2.4 ps.[7,8,17,18] Very recently, low-intensity pump−probe measurements at 77 K have shown a 1.2 ps B800 to B850 time scale.[11] The extent of B800−B800 transfer prior to B800−B850 energy transfer is not clear, but low-temperature steady state emission polarization and some hole burning studies of B800 have been interpreted as indicating that such transfer does occur.[15,17] Transient absorption experiments on B800 reveal a 400 fs decay component which has been interpreted as either vibrational relaxation[8,12] or intraband energy transfer.[11] Very recently, transient grating and three pulse photon echo spectroscopies have been used to study B800 dynamics at room temperatures.[12] These studies have provided both the spectral density of protein fluctuations coupled to the optical transition and an estimate of the B800 homogeneous bandwidth, which is calculated to be 220 cm^{-1} at room temperature. The echo results also point to

* Author to whom correspondence should be addressed.
[⊗] Abstract published in *Advance ACS Abstracts,* March 15, 1996.

0022-3654/96/20100-6825$12.00/0

the absence of <1 ps time scale intraband energy transfer at room temperature.

Until recently, very few studies of the B850 band have been performed with time resolved spectroscopies. The lifetime of the B850 excited state in isolated complexes is ~600 ps.[16] Picosecond time resolved studies were unable to resolve the emission depolarization, indicating that excited state dynamics occur on a subpicosecond time scale. In contrast to findings on B800, where the band is found to be mainly inhomogeneously broadened, hole burning studies of B850 have shown that at low temperature the exciton bandwidth is ~220 cm^{-1} and the "inhomogeneous bandwidth" is only 60 cm^{-1}.[18,19] We will consider the meaning of this inhomogeneous bandwidth in connection with our model for energy transfer in B850. Furthermore, satellite holes are found at 280, 340, 560, 750, and 920 cm^{-1} blue shifted from the zero phonon hole. These holes are interpreted as vibronic satellite holes because high-resolution fluorescence excitation spectra of BChl*a* at 5 K show almost identical frequencies.[21] As of yet, experimental studies have not shown the time scale of transfer within the B850 band. The mechanism of energy flow within B850 is unclear, because the crystal structure highlights a situation in which Förster theory would seem to be inadequate for describing the process. Exchange and charge transfer interactions similar to those in the reaction center special pair may dominate, and the magnitude of the electronic coupling may be poorly determined by a dipole−dipole approach.[20,22,23] Furthermore, using an incoherent hopping description may underestimate the rate at which energy circulates in ringlike aggregates.[24,25] For example, Kenkre has used a generalized master equation treatment to show explicitly for the case of a four site ring that excitation transfer will occur between pigments which are not connected by matrix elements of the electronic interaction.[24]

Energy transfer dynamics within the LH1 complex of *Rb. sphaeroides* have recently been studied in detail with subpicosecond spontaneous emission measurements in our laboratory.[26] In those measurements, the fluorescence anisotropy was found to decay from an initial value near 0.4−0.07 with a biphasic decay characterized by time constants of approximately 110 fs (60−75%) and 400 fs (25−40%). The non-exponential decay could be explained by either a symmetric ring structure for the antenna with an inhomogeneous spectral distribution function for the pigments or by a ring structure in which the pigments are clustered. Furthermore, oscillations were found in the isotropic emission with 105 cm^{-1} frequency, whose damping time (350−500 fs) is slower than the dominant depolarization time scale. These oscillations originate from coherent nuclear motion in the excited state. Using a model of hopping between dimers, based on the available structural information for LH1,[3] gives a hopping time of 80 fs. The observation that the damping time for the oscillations is longer than the hopping time implies that coherence transfer must be included in the description of the dynamics.[27]

This article presents results from subpicosecond spontaneous emission measurements of detergent isolated LH2 complexes. Isotropic signals reveal interband dynamics by monitoring the appearance of an emitting species. In contrast, emission depolarization is a probe of intraband dynamics since it monitors the scrambling of the initially excited orientations in a sample. Furthermore, since we measure only spontaneous emission, we isolate the excited state dynamics of the chromophores. These measurements directly reveal the time scale of energy migration dynamics within the B850 band and between the B800 and B850 pigments of the LH2 complex.

TABLE 1: Fits for B850 Isotropic Measurements

sample	$\lambda_{ex}/\lambda_{det}$ (nm)	τ_{rise} (fs)	τ_1 (ps)	A_1 (%)	τ_2 (ps)	A_2 (%)	τ_3 (ps)	A_3 (%)
BOG	840/940	46	1.7	30	14	52	~600	18
	850/940	41	3.6	46	24	34	~600	20
	860/940		1.6	36	22	55	~600	8
LDAO	850/950		0.94	35	7.2	43	~600	22

II. Experimental Section

LH2 complexes were isolated from wild type *Rb. sphaeroides*. Chromatophores were suspended in 0.01 M Tris/0.01 mM EDTA buffer and LH2/LH1/reaction centers were separated by extraction with 2% *N*-octyl-β-D-glucopyranoside (BOG)/0.1% NaCl and ultracentrifugation. The supernatant was subjected to fractional ammonium sulfate precipitation, and the earliest fractions were judged to contain only LH2 according to the absorption spectrum. The precipitate was dissolved in a minimal quantity of 0.8% BOG and then dialyzed against 0.8% BOG overnight. The LH2 was then loaded onto a DEAE-cellulose column, washed with 0.8% BOG/0.1 M NaCl, and eluted by increasing the NaCl concentration to 0.2 M. Complexes solubilized in lauryl dimethylamine oxide (LDAO) were also studied. For fluorescence up-conversion measurements, the optical density of the samples was typically adjusted to 1.0/mm. The isotropic emission kinetics were found to be independent of optical density in the range from 0.4 to 1.5/mm.

The laser source and optical arrangement for the fluorescence up-conversion experiments have been described previously.[26,28] The excitation pulses were provided by a tunable, mode-locked titanium:sapphire laser (Coherent Mira 900F) operating at 76 MHz repetition rate. The optical arrangement utilizes conventional lenses for focusing of the gate and excitation beams, whereas the spontaneous emission is focused by an elliptical mirror arrangement in which the sample cell is placed at one focus of the ellipse and the up-conversion crystal (0.5 mm BBO; Type I) is located at the other focus. The instrument response function (IRF), as measured by the cross-correlation of the excitation beam with the gate beam, is 160 fs full width at half-maximum (fwhm). The bandwidth of the pulses is 10 nm fwhm. The ~8 nm up-converted bandwidth of fluorescence is passed through a 10 nm bandpass filter and a double monochromator and detected by a photomultiplier tube. Excitation and gate beams passed through 1 cm calcite polarizers and the polarization of the excitation beam was rotated with a quartz zero-order wave plate located downstream of the polarizer. All experiments were performed with 0.4 nJ/pulse excitation. The sample was flowed with either a peristaltic pump or impeller pump through a 1 mm path-length quartz cell. The 5 mL sample volume was cooled with ice water.

To verify that accurate polarization measurements can be made with this optical arrangement, the fluorescence anisotropy of the dye IR132 was measured to be 0.39 ± 0.02. It was noted that the excitation energy must be kept very low (less than 0.5 nJ/pulse) in order to achieve correct anisotropy values at this high repetition rate.

III. Results

A. B850 Measurements. The B850 band was excited at 840, 850, and 860 nm, and emission was observed at 940 nm for the BOG preparation. A measurement of the LDAO preparation with excitation at 850 nm, and observation at 950 nm was also performed. The results of multiexponential fits to the isotropic emission data are summarized in Table 1. The B850 emission is seen to decay with three time constants, which

we discuss below. Furthermore, excitation at 840 and 850 nm results in a ∼50 fs rise time in the BOG preparation, whereas excitation at 860 nm does not result in a rise time. In contrast to our findings with LH1 under the same conditions,[26] we see no evidence for oscillations in the emission signals.

The reduction of the excited state lifetime of antenna complexes due to singlet−singlet and singlet−triplet annihilation processes has already been observed and discussed at great length. We will summarize the findings from our previous work on the LH1 antenna.[26] The time constants and amplitudes found here are similar to those found for LH1 annihilation processes (compare Table 1 of this work with Table 1 of ref 26). In that work, we combined simulations with variable intensity measurements to enable identification of the two annihilation time scales. By performing up-conversion measurements at reduced repetition rate (250 kHz) so as to eliminate the accumulation of triplet states, we were able to assign the ∼1 ps time scale component to singlet−singlet annihilation. With a simple calculation, taking into account the fraction of excited complexes per pulse (about 20%), the repetition rate of the laser (76 MHz), a triplet lifetime of 3 μs, and a triplet yield of 2%, we show that the steady state triplet population is about 50%. This value is in reasonable agreement with the observed amplitude of the second annihilation time scale. We conclude this to be the time scale for singlet−triplet annihilation. By analogy with the LH1 work, we therefore identify the ∼1 and 14−23 ps components as arising from singlet−singlet and singlet−triplet annihilation, respectively. The singlet−triplet annihilation time scale is significantly longer than that observed in LH1, from which we can only conclude that the annihilation is less efficient in LH2. The wavelength variation of the fastest decay component in the BOG preparation may reflect spectral evolution occurring on the same time scale as singlet−singlet annihilation. The variation probably also reflects the difficulty of uniquely fitting data sets with three decay components. Despite the wavelength variation, there seems to be a significant difference in the fast decay time constant between the LDAO and BOG preparations. As discussed in recent work on LH1,[26] the singlet−singlet annihilation time in these complexes is migration limited and is thus proportional to the square of the number of pigments in the domain. In contrast, the singlet−triplet annihilation is trap limited and scales linearly with the number of pigments. Therefore, the difference in the rates of the two annihilation processes may indicate that the complex size in the BOG preparation is larger than that in the LDAO preparation. This result indicates the need for care in comparing the results of different experiments on these complexes, since the isolation procedure may alter the number of pigments within the complex. It is well-known that attempts to crystallize the LH1 complex are hampered by the finding that the samples are not monodisperse; complex sizes from 12 to 32 pigments have been observed in various studies.[3,29] In contrast, light scattering experiments show that detergent preparations of LH2 seem to be monodisperse over a wide range of conditions.[30] For the purposes of our analysis, we will assume that our LH2 samples prepared in BOG contain the same number of pigments as the LH2 crystals in ref 2, which were prepared in the same detergent.

The intraband B850 dynamics were studied with polarized upconversion measurements by measuring emission parallel and perpendicular to the excitation polarization. Polarized emission data for the LDAO preparation are shown in Figure 1. The anisotropy was reconstructed by the method of Cross and Fleming.[31] The isotropic data are fit independently, and the fit is used as the input for a scheme in which parallel and perpendicular emission components are simultaneously fit,

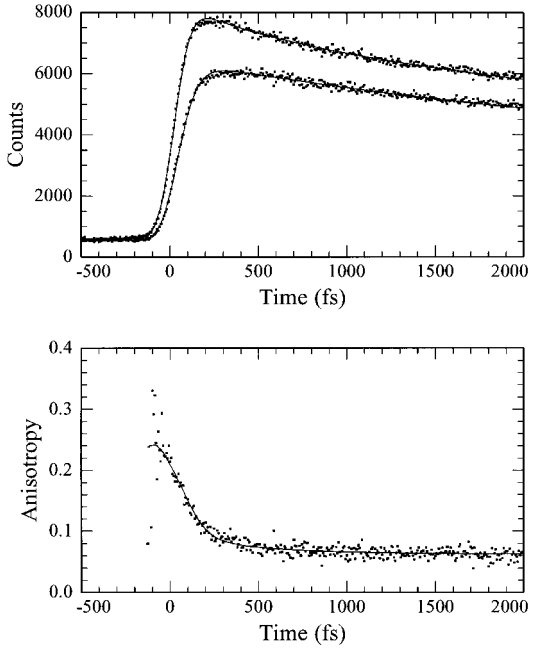

Figure 1. (Top) Polarized, time resolved emission from LH2/LDAO: excitation at 850 nm and detection at 940 nm. The emission parallel (upper) and perpendicular (lower) to the excitation pulse polarization is rendered in dots, and the simultaneous fit is shown in solid lines. The fit parameters are shown in Table 2. (Bottom) The raw experimental anisotropy function (dots) along with the same function derived from the fitted convoluted parallel and perpendicular curves (solid).

TABLE 2: Fits for Anisotropy

sample	$\lambda_{ex}/\lambda_{det}$ (nm)	r_1	τ_1 (fs)	r_2	τ_2 (fs)	r_∞
BOG	840/940	>0.2	∼40−50	.06	320	.06
	850/940	.18	82	.05	330	.06
	860/940	.21	90	.04	410	.08
LDAO	800/900	.20	45	.09	350	.07
	850/950	.21	50	.04	520	.05

assuming the depolarization follows a multiexponential form. The anisotropy decays on two subpicosecond time scales (less than 100 and 300−500 fs), which are wavelength dependent. The anisotropy fit parameters are listed in Table 2. Overall, the results are very similar to the LH1 depolarization. The initial phase of the depolarization is always seen to be faster than in LH1. Also in contrast to LH1, the initial phase of the decay shows some wavelength dependence, becoming faster as the excitation is tuned to the blue side of the B850 absorption band. Furthermore, the terminal anisotropy also shows a wavelength dependence; note that the final anisotropy is higher for 860 nm excitation as compared to the shorter excitation wavelengths.

B. B800 Measurements. The B800 band was excited at 800 nm, and B850 emission was detected at several wavelengths in the region 895−920 nm; no variation of the signals was observed. A typical isotropic measurement is shown in Figure 2 (900 nm detection), along with a fit. The rise time is well-fit by a single exponential, with time constant 655 fs. Decay components with time constants 2.2 ps (66%) and 600 ps (33%) are also present in longer scans. The data could also have been fit with the rise time and three decay components similar to those found for B850. The rise time directly reveals the B800 to B850 energy transfer rate and is consistent with previous subpicosecond pump−probe measurements.[8,9] Emission depolarization was also measured; the data are shown in Figure 3, and the anisotropy fit parameters are in Table 2.

Although the anisotropy of the IR132 dye at short times was measured to be 0.4 with our optical arrangement, the initial

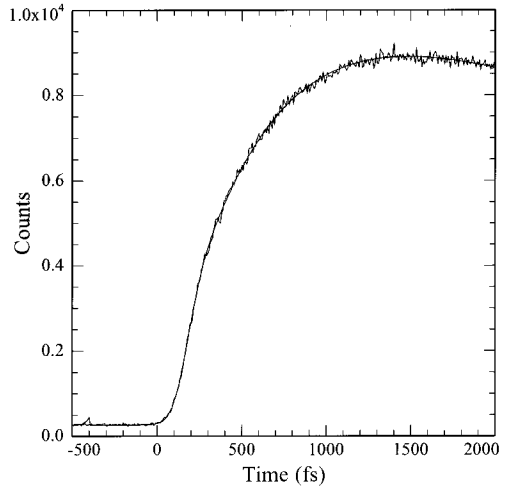

Figure 2. Isotropic B850 fluorescence (900 nm) from LH2/LDAO when B800 is directly excited. The smooth line is a fit, giving a single exponential 650 fs rise which can be identified as the B800 to B850 energy transfer.

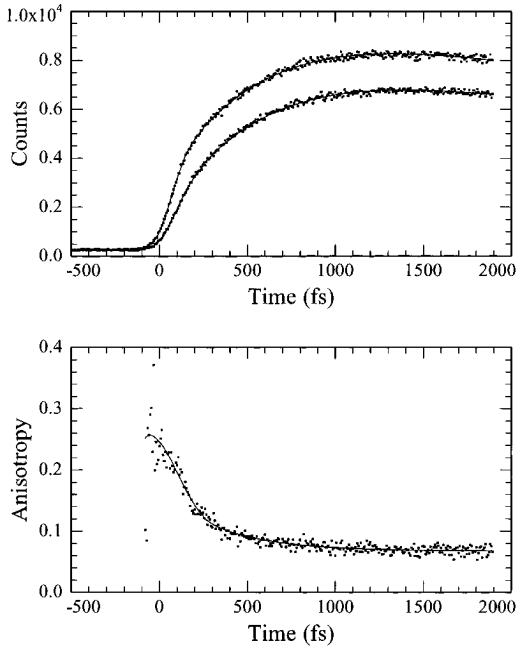

Figure 3. Polarized B850 emission subsequent to B800 excitation for LH2/LDAO: (Top) Parallel and perpendicular components (dots) and fits (solid lines); (Bottom) raw experimental anisotropy and same function derived from fitted curves (solid line). The fit parameters are given in Table 2.

anisotropy of our LH2 depolarization data falls short of this theoretically expected value. One possible reason for this effect is that the fitting procedure for the anisotropy decay critically depends on knowing the functional forms of the depolarization and the IRF. Even if an exponential depolarization process occurs on a shorter time scale than the width of the instrument response, most of the true depolarization will be recovered. However, deviations from exponential form will cause errors in determining the initial anisotropy, especially when the time scale of the decay is shorter than the width of the instrument response (see the Appendix).

IV. Discussion

We will use a Förster approach to discuss transfer between B800 chromophores and from B800 to B850. The 2.5 Å crystal structure of LH2 places rather tight constraints on the geometrical aspects of our model. Since the sizes of the BChl*a* pigments are comparable to the distances between them, the validity of the point−dipole approximation should be questioned. We address this point by the use of the point−monopole method.[32] We will attempt to interpret the B850 depolarization data in terms of hopping between dimers of BChl*a* pigments whose site energies are distributed within the B850 absorption band. This analysis is analogous to the approach used in considering the B870 band of LH1.[26] Before embarking on this, we consider whether it is reasonable to use an incoherent dimer hopping model. We describe a model for B850 as a disordered, excitonically coupled aggregate and consider its properties. Then we will attempt to reconcile the exciton model with the hopping model.

A. Exciton Model for the B850 Pigments. The B850 chromophores may be conceptualized as a symmetric circular aggregate of N BChl*a* molecules. The exciton level structure of circular aggregates is well-known.[33,34] If the coupling between pairs of adjacent chromophores is the same and we consider only the lowest excited electronic state of each molecule, the electronic eigenstates are split into N levels ($N = 18$), labeled $k = 0, \pm1, \pm2, ..., 9$. The exciton states can be written as linear combinations of monomer wave functions,

$$|\Psi_k\rangle = \sum_{n=1}^{N} b_{kn}|n\rangle \tag{1}$$

and the energy levels are

$$E_k = E_{\mathrm{BChl}a} + 2U\cos(2\pi k/N) \tag{2}$$

where $E_{\mathrm{BChl}a}$ is the energy of the monomeric BChl*a* and U is the electronic coupling. The $k = 0$ and $k = 9$ levels are nondegenerate, but the intervening levels are doubly degenerate. A more realistic description of LH1 and LH2 is an arrangement in which the pigments are segregated into N groups of M pigments, into overall C_N symmetry. Here, the N exciton levels are further split into M branches. For bacterial antenna the structures suggest $M = 2$, since the spacing between chromophores alternates. In particular, if we use an electronic coupling $U_{\alpha\beta}$ between BChl*a* monomers within an $\alpha\beta$ unit and $U_{\alpha\beta-\alpha\beta}$ for coupling between BChl*a* on neighboring monomers across units, we find the lowest energy level at $E_{\mathrm{Bchla}} - U_{\alpha\beta} - U_{\alpha\beta-\alpha\beta}$, whereas the highest level is $E_{\mathrm{BChl}a} + U_{\alpha\beta} + U_{\alpha\beta-\alpha\beta}$. The transition dipole moment from the ground state to each level is

$$\boldsymbol{\mu}_k = \sum_{n=1}^{N} b_{kn}\boldsymbol{\mu}_n \tag{3}$$

If the antenna is perfectly homogeneous and $U_{\alpha\beta-\alpha\beta} = U_{\alpha\beta}$, only transitions to $k = \pm1$ levels are dipole allowed from the ground state. If $U_{\alpha\beta-\alpha\beta} \neq U_{\alpha\beta}$, then $k = \pm1$ and $k = \pm8$ are allowed, but $k = \pm8$ are weak if the subunits are head-to-head or head-to-tail dimers. When inhomogeneity is introduced into the system ($E_{\mathrm{BChl}a}$ is replaced by a distribution of site energies), the absorption spectrum becomes slightly more complicated because degeneracies are removed and transitions to all exciton states gain oscillator strength. We will treat the exciton levels and inhomogeneity for the case of diagonal disorder using the same approach as Fidder et al.[32] For LH2, the exciton Hamiltonian may be written as

$$H = \begin{bmatrix} E_1 & U_{\alpha\beta} & & & & & U_{\alpha\beta-\alpha\beta} \\ U_{\alpha\beta} & E_2 & U_{\alpha\beta-\alpha\beta} & & & & \\ & U_{\alpha\beta-\alpha\beta} & E_3 & U_{\alpha\beta} & & 0 & \\ & & & \ddots & & & \\ & & & U_{\alpha\beta} & E_{N-2} & U_{\alpha\beta-\alpha\beta} & \\ & 0 & & & U_{\alpha\beta-\alpha\beta} & E_{N-1} & U_{\alpha\beta} \\ U_{\alpha\beta-\alpha\beta} & & & & & U_{\alpha\beta} & E_N \end{bmatrix} \quad (4)$$

where E_n is the site energy of the nth BChl*a*. We assume the site energies follow a Gaussian distribution centered on $E_{\mathrm{BChl}a} = 11\,968$ cm^{-1}. We select these energies with a Monte-Carlo scheme. The Hamiltonian is diagonalized numerically in order to solve for the energy levels and eigenstates. We perform an average over 5000 Monte-Carlo iterations in order to sample the energy distribution adequately. The absorption spectrum resulting from a calculation which includes a 200 cm^{-1} fwhm distribution of site energies, along with $U_{\alpha\beta} = 230$ cm^{-1} and $U_{\alpha\beta-\alpha\beta} = 110$ cm^{-1} is shown in Figure 4. For this example, we have fixed the intradimer coupling, $U_{\alpha\beta}$, to the experimental value for coupling in the dimeric B820 subunit of LH1.[45] The interdimer coupling, $U_{\alpha\beta-\alpha\beta}$, is determined by assuming an exponential distance dependence of the coupling strength,[22] with parameters from ref 35. Assuming an exponential distance dependence of the coupling seems to be reasonable for exchange interactions.[29] As we discuss below, our conclusions are mostly sensitive to the magnitude of disorder relative to the values of both $U_{\alpha\beta}$ and $U_{\alpha\beta-\alpha\beta}$ rather than the ratio of the coupling strengths.

As a result of the lack of extremely distinct spacing between successive pairs of chromophores, the arrangement of the B850 bacteriochlorophylls does not easily lend itself to visualization in terms of dimers. However, the coupling strengths may significantly alternate because very small differences in spacing between the chlorin rings may cause "tuning" of the absorption wavelength. For example, it was calculated that the blue shift of the *Rb. sphaeroides* special pair absorption (870 nm) relative to that of *Rps. viridis* (960 nm) may be the result of a difference of only 0.2−0.3 Å in spacing between the rings, which is observed in the crystal structures.[23,36,37] Of course, electronic structure calculations of B850 are necessary to confirm this speculation.

Experimentally, there is evidence that delocalized exciton states exist at low temperatures. Hole burning action spectra of LH2 show that the lowest energy feature in the B850 band peaks at 870 nm (11 480 ± 20 cm^{-1}) with a width of 60 cm^{-1}. The zero-phonon hole of B850 has a width of 3.2 cm^{-1}, which corresponds to a homogeneous lifetime of 6.6 ps.[19] Small and co-workers argue that the best explanation for the narrow hole at 870 nm is the presence of the lowest energy exciton component ($k = 0$) of the B850 band, which gains oscillator strength as a result of energetic disorder. The inhomogeneous width of 60 cm^{-1} corresponds to the broadening of the $k = 0$ exciton level due to site inhomogeneity. In ref 26, we noted that exchange narrowing must be considered for the B870 and B850 aggregates in appraising this width if the excitation is delocalized. Delocalization will lower the observed inhomogeneity in the low-temperature absorption spectrum compared to the distribution of site energies. A site inhomogeneous distribution width of ∼200 cm^{-1} leads to an effective width of 60 cm^{-1} for the $k = 0$ level (also in Figure 4), as seen in Reddy *et al.*'s action spectrum. As discussed by Fidder and co-workers,

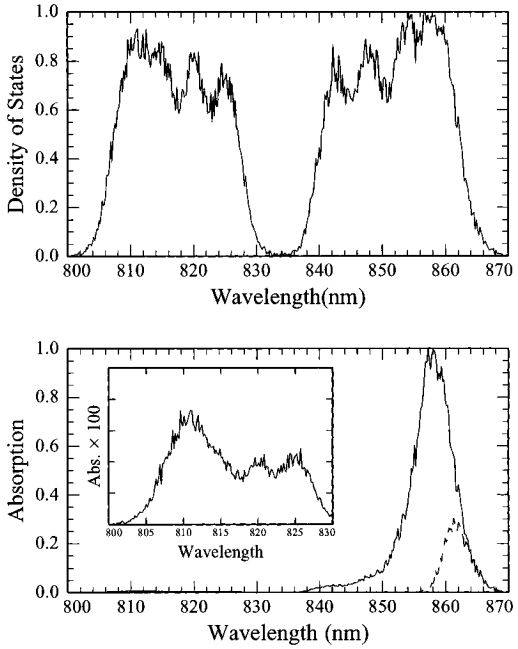

Figure 4. Results of exciton calculations for B850 based on the crystal structure. Hamiltonian and parameters are given in the text. (Top) Density of excitonic states. The resolution of the spectrum is 3.4 cm^{-1}. (Bottom) Absorption spectrum. The calculated $k = 0$ line shape appears with a dashed line. The states lying at the high-energy side will have good overlap with B800 emission.

if the magnitude of disorder (D, the standard deviation of the Gaussian distribution) is comparable to the electronic coupling ($D/U \sim 0.5$), the electronic eigenstates will become localized.[33] An "inverse participation ratio" or localization parameter, $L(E)$, indicates the extent of delocalization for the states at energy E:

$$L(E) = \frac{1}{N\rho(E)}\langle\sum_k \delta(E - E_k)(\sum_n b_{kn}{}^4)\rangle \quad (5)$$

In this expression, N is the number of molecules comprising the aggregate, $\rho(E)$ is the density of states at energy E, E_k is the energy eigenvalue for each of the k exciton states, n labels the individual BChl*a* molecules, and b_{kn} is the coefficient for each monomer wave function in that exciton state. For B850, the function $L(E)$ can range from a value of $^1/_{18}$ for a fully delocalized state, through 0.5 for a dimer, to a value of 1.0 for a state localized on a single BChl*a*. The localization function calculated for our model of B850 is plotted in Figure 5. Our calculation shows that for states with significant oscillator strength, the excitation is delocalized over ∼5 pigments at low temperatures (compare with the absorption spectrum in Figure 4). Our model Hamiltonian does not include phonons, which we expect will further localize the electronic eigenstates at higher temperatures. Even if the electronic states are partially delocalized, a hopping model may correctly determine the center of mass motion of the exciton. A full theoretical approach to the problem of coupled coherent−incoherent excitation migration which includes energetic disorder and a spectral density of fluctuations for the bath has not yet been developed. Finally, note that our model for B850 only includes energetic (diagonal) disorder. Off-diagonal (structural) disorder will further localize the electronic eigenstates.[33] However quantitative estimates of the amount of structural disorder in LH2 are not yet available. These considerations lead us to suggest that a reasonable zeroth order model for B850 is a ring of dimers with energy migration occurring via a hopping mechanism.

B. Weak-Coupling, Incoherent Transfer Models. In general, any weak-coupling rate of electronic excitation transfer

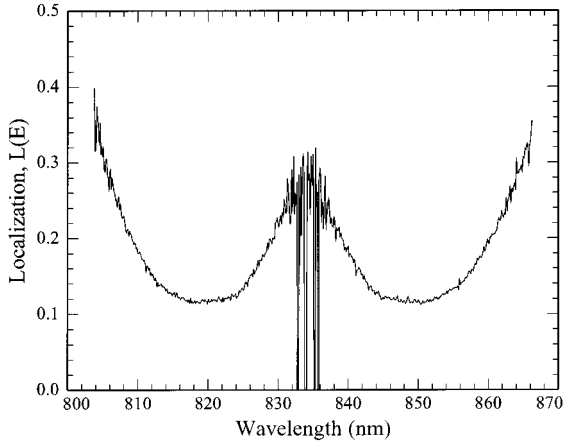

Figure 5. Calculation of the inverse particpation ratio, eq 5, for B850. A value of 0.5 indicates localization on a dimer, whereas a value of 0.1 indicates delocalization over ~10 BChla.

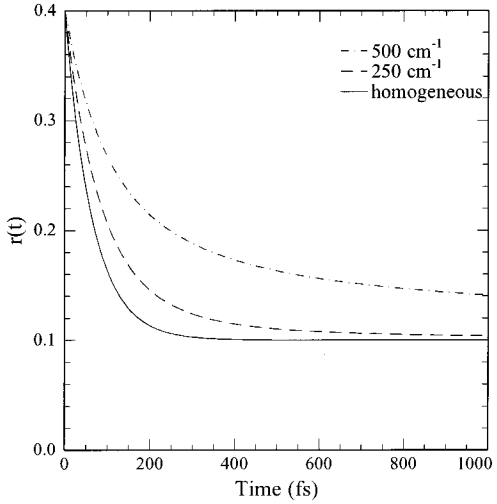

Figure 6. Simulated B850 depolarization based on the crystal structure and three different values for the inhomogeneous distribution of site energies within the B850 band. Exponential fit parameters are collected in Table 3.

can be written as

$$K_{ET} = \frac{4\pi^2}{h}|U|^2 S \qquad (6)$$

where S is the spectral overlap and U is the excitation interaction matrix element. This excitation coupling (U) is the same interaction that in the strong-coupling limit is responsible for exciton splitting of the spectra (e.g., $U_{\alpha\beta-\alpha\beta}$ for hopping between dimers in B850).[38] The total electronic interaction is the sum of exchange and Coulombic contributions. Here, we ignore charge transfer interactions, although these may be important for chromophores in very close contact such as the B850 BChl*a*. For the case of pure exchange interactions the energy transfer proceeds via the Dexter mechanism.[39] When the separation between the chromophores approaches the size of the molecules (for BChla, Mg−Mg separations less than ~20 Å), the shape of the molecular charge distribution must be considered for the Coulombic term. A method for calculating the total excitation interaction as a sum of electrostatic interactions between point monopoles located at the atoms of the donor and acceptor has been developed.[32] In order to assess the importance of higher order Coulombic interactions, we have performed point monopole calculations for the B850 chromophores using the parameters from Chang.[32] Coordinates for BChl*a* were taken from the accessory BChl*a* of the *Rb. sphaeroides* reaction center crystal structure;[36] positions and orientations for the BChl*a* were taken from the LH2 crystal structure.[2] For BChl*a* bound to the same $\alpha\beta$ polypeptide pair, the full monopole interaction is 236 cm^{-1}, whereas the dipole−dipole value is 286 cm^{-1}. For adjacent BChl*a* on neighboring polypeptide pairs, the monopole interaction is 178 cm^{-1} as compared to 202 cm^{-1} for the dipole−dipole value. The Q_y electronic transition of BChl*a* has large oscillator strength, therefore, we expect much of the coupling to result from Coulombic interactions rather than exchange interactions. The magnitude of the charge transfer coupling is unknown. Although these calculations do not reveal as large a distinction between intradimer and interdimer coupling strengths as we use for our excitonic model of B850, we do not expect our conclusions to be affected: when the magnitude of disorder is comparable to the electronic coupling, the eigenstates are localized even if the coupling strength alternation is less pronounced. As demonstrated here, the monopole corrections only amount to 20% or less.

Most commonly, the case of purely Coulombic interaction is considered; at large donor−acceptor separations the interaction can be well-approximated as point dipole−dipole (Förster theory). Using Förster theory, and geometric parameters from the X-ray structure, we can calculate the energy transfer rates if we make some assumptions about the form of the spectral overlap integral. The Förster formula can be written[38]

$$K_{ET} = \frac{9 \ln 10 \kappa^2 c^4 \mu_A^2 \mu_D^2}{128\pi^5 \eta^4 R^6} \int \epsilon_A(\nu)\, F_D(\nu)\, d\nu \qquad (7)$$

where ν is the frequency, $\epsilon_A(\nu)$ is normalized absorption spectrum of the acceptor, $F_D(\nu)$ is the normalized emission spectrum of the donor, η is the refractive index of the medium, κ^2 is the orientation factor, c is the speed of light, μ_D and μ_A are the integrated dipole strengths of each chromophore, and R is the Mg−Mg separation between the donor and acceptor. The spectral overlap integral is not easy to determine accurately for various reasons to be discussed below. If we assume Gaussian absorption and emission spectra, the overlap integral can be written analytically:[40]

$$S = \frac{1}{2\pi^{1/2}\sigma_D\sigma_A}\left(\frac{1}{2\sigma_D^2} + \frac{1}{2\sigma_A^2}\right)^{-1/2} \times \exp\left[\frac{-\Delta^2}{4\sigma_D^2\sigma_A^2}\left(\frac{1}{2\sigma_A^2} + \frac{1}{2\sigma_A^2}\right)^{-1}\right] \qquad (8)$$

where σ's are the standard deviations of the bandwidths (fwhm/$(8 \ln 2)^{1/2}$) and Δ is the difference between the maxima of the two bands. The integral from expression 7 can be replaced with the value calculated from this expression. Förster has clearly stated that the overlap integral is to be evaluated as a means of quantifying the role of vibrations in the energy transfer; he explicitly calls it a vibronic overlap integral.[38] Therefore only the homogeneous line shape should be used for evaluating these integrals. Using observed absorption and emission bandwidths can lead to an egregious overestimate of the excitation transfer rate.

Our data show that the time scale of B800 to B850 transfer is 650 fs, independent of any structural model. The B850 depolarization shows biexponential decay on a sub-100 fs time scale and a 400−500 fs time scale. The connection between the depolarization time scales and hopping time scales can easily be understood for a ring structure. Consider a system of N identical chromophores (each may be a single BChl*a* molecule

or a dimer) arranged symmetrically in a ring where the dipoles lie in a plane and the excitation migrates from one chromophore to another with time constant τ_{hop}. In this type of structure the anisotropy will decay from an initial value of 0.4 to a terminal value of 0.1 with a single exponential time constant, τ_{depol}. This time constant is related to the hopping time and the symmetric structure via

$$\tau_{depol} = \frac{\tau_{hop}}{4(1 - \cos^2 \theta)} \tag{9}$$

where $\theta = 360°/N$ is the angle between the dipoles of adjacent chromophores on the ring. Equation 9 can be understood by considering that depolarization is complete when the transition dipole migrates through 90° and by considering how many hops are required for this rotation to be accomplished. However, a non-exponential depolarization will result from a distribution of rates when the chromophore site energies are distributed.[26] When there is a distribution of pigment site energies, the depolarization must be simulated numerically. We will follow this approach for the B850 depolarization.

C. Interpretation of the Results. *1. B800 to B850 Excitation Transfer.* Previous studies have provided evidence that the B800 to B850 energy transfer step occurs via a Förster mechanism. The structural information affords us a more precise test. Sundström and co-workers have performed low-temperature (77 K) femtosecond pump−probe measurements on a series of LH2 complexes in which the absorption maximum of the B850 band varies over the range of 826−850 nm.[7] They find that the low-temperature transfer rate over the temperature range from 1.2 to 77 K is 2.4 ps. The spectral overlap dependence of the rate in the series of mutants is found to be approximately consistent with a weak coupling Coulombic mechanism. In a more recent study utilizing very low intensity transient absorption spectroscopy at 77 K, van Grondelle and co-workers measure a value of 1.2 ps for the B800 to B850 transfer time.[11] They find that increasing the light intensity leads to irreversible photodamage which increases the B800 to B850 transfer time to 2.4 ps. Our result demonstrates a room temperature transfer time of 650 fs, in close agreement with the findings in refs 8, 9, and 12. These findings suggest that B800 to B850 transfer slows by only a factor of 2 in cooling from 300 to 1.2 K (in which kT changes by a factor of 200). Small suggests that the temperature invariance of the transfer rate results from the B850 homogeneous line being determined by the excitonic bandwidth; therefore the spectral overlap with B800 is temperature independent up to 77 K.

In order to interpret this time scale, we will assume excitation transfer from a monomeric B800 pigment to a dimeric B850 chromophore. We use a single Gaussian absorption spectrum for the B850 dimer rather than the spectrum in Figure 4, which includes inhomogeneous broadening. As discussed above, homogeneous line shapes should be used for a proper calculation of transfer rates. Photon echo experiments are useful for providing an estimate of the homogeneous bandwidth. Here, we make use of the B800 homogeneous bandwidth determined by Joo *et al.* (220 cm^{-1} fwhm).[12] The other parameters we use for calculating the B800 to B850 rate are the experimentally observed B800 Stokes shift (5 nm),[14] the B800 to B850 center-to center distance and relative orientations from the crystal structure (17.6 Å, parallel Q_y transition dipoles), a Gaussian B850 absorption centered on 850 nm with a fwhm of 250 cm^{-1},[46] and transition dipole moments of 41 D^2 for B800 and 76 D^2 for B850 (assuming a head-to-head or head-to-tail BChla dimer).[45] These parameters give transfer times around 18 ns; these values are many orders of magnitude slower than the observed rates. However, there is at least one serious error in our calculation which may cause us to underestimate the transfer rate to dimeric B850: we are assuming that both donor and acceptor homogeneous line shapes are Gaussian without including vibronic bands that would cause the spectra to be multiply peaked. A sum of Gaussian lines for B800 and B850 does not reproduce the LH2 absorption spectrum. In B850 hole burning, Small and co-workers observe vibronic satellite holes of B850 at various frequencies.[18] In particular, Small *et al.* implicate the 750 cm^{-1} mode as being involved in B800 to B850 transfer, since it has good overlap with the B800 emission band. Using one Gaussian to represent this vibronic line (located at 800 nm) with a 250 cm^{-1} bandwidth, and a Franck−Condon factor of 0.05 [18] gives a transfer time of 7.5 ps. This value is only a factor of 10 slower than the observed rate. A more accurate calculation including one or two more vibronic lines could easily bring the calculated rate into agreement with the observed rate. The position of this vibronic line may result in a weak temperature dependence; invariance of the rate results if the donor and acceptor spectra are completely overlapped. Of course, another possibility we need to consider is energy transfer from B800 to the upper exciton component of the B850 dimer (see Figure 4), rather than just to the lower level. The results of our exciton calculation show that the upper exciton state of the B850 dimer lies at ∼815 nm, partially overlapping the B800 emission at 805 nm. At this point, it seems that transfer into this exciton state of B850 cannot be ruled out. Although we have discussed transfer into either a B850 vibronic level or excitonic level, note that these possiblities are not mutually exclusive. Excitation transfer from B800 to B850 occurring through the higher lying exciton state would be analogous to what has been proposed for energy transfer from the accessory bacteriochlorophyll to the special pair of the reaction center.[40,42] The distinction between transfer into a vibronic or excitonic level can be experimentally addressed by polarized transient absorption experiments on B850 since transfer into the exciton states may give rise to different polarization behavior than transfer into an excited vibrational level.

2. B800 to B800 Excitation Transfer. If we use Förster theory to calculate the B800 to B800 energy transfer rate with 22 Å interchromophore distance, an orientation factor $\kappa^2 \sim 3.55$ from the structure, and the same spectral parameters as above, we obtain transfer times on the order of 1.25 ps. Despite the large separation between pigments, the B800 to B800 rate is fast because the band has a small Stokes shift.[14] Even if the spectra have non-Gaussian tails, the main portions of the peaks overlap so much that the use of Gaussian band shapes in our calculation is likely to be a good approximation for the region of spectral overlap. Using transition monopoles to calculate the excitation interaction increases the rate by <20% at these separations. Thus, this calculation shows that B800 to B800 energy transfer is competitive with depopulation of B800.

Now we need to consider how intraband transfer would manifest itself in the depolarization. Our data show that depolarization of the B850 emission subsequent to B800 excitation is similar to that observed upon direct excitation in the blue side of the B850 band (Table 2). In particular, note that the initial value of the anisotropy is rather high ($r(0) > 0.35$). This observation indicates that the B800 and B850 transition dipoles are nearly parallel, consistent with the structure. In Appendix 1, we show, by simulating the depolarization and by fitting of data with simulated noise, that our data sets for B800 excitation/B850 detection do not reliably yield information on the time scale of B800 to B800 excitation transfer. However, we will consider previous experimental studies and their conclusions in relation to our calculated transfer rate.

A variety of views on the time scale of B800 to B800 transfer have been expressed. There have been three experimental reports which place a time scale on the process and one which concludes that very little B800 to B800 occurs. In hole burning studies of B800 at 1.2 K, De Caro and co-workers have observed a wavelength dependence of the hole width.[17] They find the hole width to remain constant over the region 805−799 nm but find that it increases linearly as the wavelength is tuned from 799 to 789 nm. This increase in hole width is interepreted to be the result of downhill B800 to B800 energy transfer in the high-energy side of the absorption band, prior to B800 to B850 transfer. Assuming that the rate of B800 to B850 transfer is constant over the entire band, they determine a B800 to B800 transfer time of 850 fs from their hole width. In 77 K transient absorption experiments analogous to the hole burning, Monshouwer and co-workers found a 700 fs time scale for B800 to B800 energy transfer on the high-energy side of the B800 absorption band.[11] Recently, Hess and co-workers have interpreted their polarized pump−probe measurements to reveal a 300 fs B800 to B800 transfer time at 77 K.[44] In contrast to the linear spectroscopic studies mentioned above, three pulse photon echo experiments have been used to study B800 at room temperature.[12] The three pulse echo peak shift closely follows the correlation function of the optical transition frequency, thereby revealing the time scale of dynamics within the B800 band. The experimentally accessible time window is limited by depopulation of B800, so dynamics on time scales longer than about 700 fs will not be readily apparent. The echo results have been interpreted as indicating that B800 to B800 transfer does not occur prior to B800 to B850 transfer. This interpretation of the peak shift measurement seems to contradict the results of Monshouwer *et al*. and Hess *et al*. However, note that the echo data were collected at room temperature, whereas the pump−probe studies were performed at 77 K.

Another approach to finding the intraband B800 excitation transfer rate is to consider the B800 emission anisotropy. The low-temperature steady state emission anisotropy of B800 itself has been measured to be between 0.05 and 0.07.[15] Kramer *et al*. suggest that the rate of excitation transfer among B800 must significantly exceed the B800 to B850 rate in order for this value of B800 emission polarization to be attained. The B800 to B800 hopping rate can be calculated from this value of the polarization. If we assume that B800 to B800 transfer and B800 to B850 transfer occur as a single-exponential processes, the steady state polarization, r_{ss}, can be written analytically:

$$r_{ss} = \frac{0.3}{\tau_{ET}}\left(\frac{1}{\tau_{depol}} + \frac{1}{\tau_{ET}}\right)^{-1} + 0.1 \qquad (10)$$

Here, τ_{ET} is the time constant for B800 to B850 transfer, and τ_{depol} is the depolarization time scale as defined in eq 9. At 4 K, low-intensity hole burning measurements show τ_{ET} to be 2.5 ps;[17] the value of τ_{depol} which results is 370 fs. Since there are 9 B800 BChla, the hopping time is thus $1.653\tau_{depol} = 610$ fs. This value is shorter than that calculated above from Förster theory for room temperature hopping and is consistent with the values derived by De Caro *et al.* from their hole widths on the high-energy side of the absorption band.[17] Steady state fluorescence anisotropy data for B800 are not available at higher temperatures, so we cannot follow the above analysis for 77 K or room temperature intraband transfer.

3. B850 to B850 Excitation Transfer. Following the reasoning given in section A, we choose to simulate the fluorescence depolarization of the B850 chromophores, based on the structural information, using Förster theory to calculate the rates of hopping between dimers. Solution of the Pauli master equation for the population of each of the sites is achieved numerically.[26] The depolarization dynamics are calculated numerically by angle averaging using the methodology suggested by Magde.[43] The B850 band is assumed to have a homogeneous 250 cm^{-1} Gaussian spectrum peaked at 850 nm; the emission is assumed to have a 66 cm^{-1} Stokes shift.[45] We find that the hopping time between dimers is 110 fs. The simulated depolarization is displayed in Figure 6 and shows a single exponential decay with time constant 64 fs. The depolarization has also been calculated in the case for which there is a Gaussian distribution of pigment site energies. The depolarization calculation is performed as previously described, with inhomogeneous widths of 250 and 500 cm^{-1}.[26] The results of these simulations are also displayed in Figure 6, and the results of double exponential fits are organized in Table 3. In particular, note that a 250 cm^{-1} Gaussian distribution of pigment site energies approximately reproduces the experimentally observed biexponential decay. This value of inhomogeneity is similar to that required for explaining the non-exponential decay of the LH1 depolarization and is also consistent with pump−probe studies of spectral evolution in LH1 at room temperature.[46]

TABLE 3: Exponential Fits to Simulated B850 Depolarization

inhom width (cm^{-1})	r_1	τ_1 (fs)	r_2	τ_2 (fs)	r_∞
0	0.30	64			0.10
250	0.23	76	0.07	210	0.10
500	0.20	108	0.10	1000	0.10

Experimentally, we observe the terminal anisotropy of the signal increases as the excitation wavelength increases. As mentioned above, we expect $r_\infty = 0.1$ for a homogeneous system in which the excitation is randomized in a plane.[43] The variation in final anisotropy value is consistent with a small inhomogeneous distribution combined with the effect of spectral selection in both the excitation and detection steps. Simulations show a systematic drop in $r(\infty)$ as the detection window is moved toward the red edge of the steady state emission spectrum[48] In an inhomogeneous antenna, excitation equilibration produces a nonuniform final distribution; detection removed from the excitation wavelength, on average, excludes the initially excited chromophore and consequently lowers the final anisotropy. Experimentally, we observe an equivalent effect when the excitation wavelength is tuned and the detection wavelength remains fixed. The presence of an isotropic rise time is also a result of the inhomogeneity of the B850 band. The initially excited pigments undergo energy transfer to lower energy pigments, which are preferentially observed in our detection window. Upon excitation on the red side of the band, the donors and acceptors emit at nearly the same wavelengths, thus no spectral evolution is observed.

D. Comparison of B850 with LH1. The most striking difference between B870 (LH1) and B850 is the absence in LH2 of the 105 cm^{-1} oscillations observed in LH1 isotropic emission. Sundström and co-workers have performed pump−probe studies of LH2 and LH1 with 40 fs pulses at various temperatures.[13] They find oscillations in their pump−probe signals which persist up to room temperature. Furthermore, Chachisvilis *et al.* find that the amplitude of the oscillations is much smaller in LH2 than in LH1. The damping time of these oscillations is nearly temperature independent for both LH2 and LH1. The absence of oscillations in room temperature isotropic B850 emission is consistent with Sundström's findings. In LH1, these oscillations could be interpreted as evidence for segregation of the pigment interactions into dimers. That is, we are assigning the 105 cm^{-1} oscillation to an intradimer mode, since this frequency is not

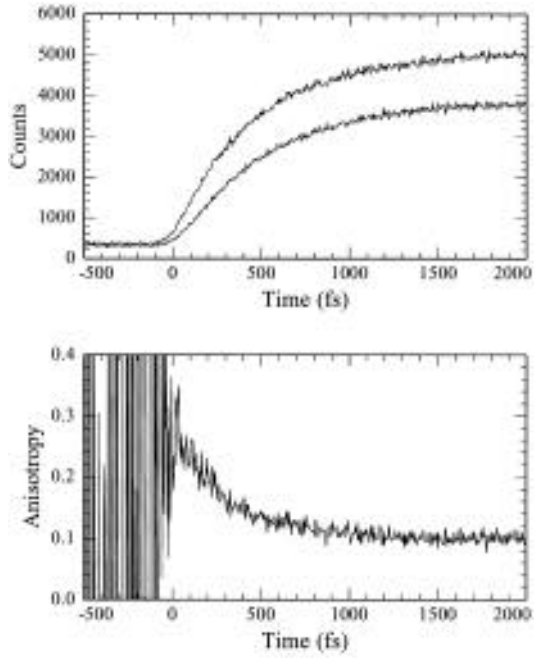

Figure 7. Simulated depolarization data with 160 fs IRF and 500 fs rise time. (Top) Parallel (top) and perpendicular (bottom) components. (Bottom). Raw experimental anisotropy. Note that the anisotropy does not seem to begin at 0.4.

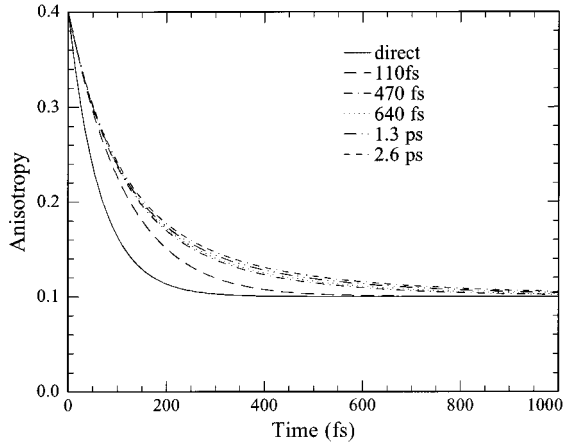

Figure 8. Simulated B850 anisotropy subsequent to B800 excitation, for various B800 to B850 transfer times. The fastest anisotropy decay is for direct B850 excitation. As the B800 to B850 transfer time increases, the depolarization slows down and reaches an asymptotic decay.

present in monomeric BChl*a*.[47] Interestingly, weak oscillations are clearly evident in the transient grating signal from B800 at room temperature,[12] where presumably the B800 is monomeric. This puzzling situation highlights the difficulty in assigning the origin of these impulsively excited vibrations to dimeric or oligomeric bacteriochlorophyll *a*.

The lack of oscillations in the fluorescence aside, we conclude by emphasizing that the emerging picture of excitation transfer in B850 of LH2 is very similar to our findings on LH1. The time scale of hopping between chromophores is very similar and so is the magnitude of energetic disorder required to describe the non-exponentiality of the depolarization. It is perhaps surprising that an incoherent hopping model adequately describes room temperature dynamics in both LH1 and LH2. However, the presence of the vibrational oscillations in LH1 indicates that a full description of the dynamics in both LH1 and LH2 will require better understanding of chromophore−protein coupling and of coherence transfer.

V. Summary

In LH2, we encounter a system in which inter- and intraband excitation transfer occurs with a fascinating combination of mechanisms. Energy transfer within the B800 band probably occurs on a 1 ps time scale, and the available data are consistent with a simple Förster description. On the other hand, energy transfer within the B850 band occurs on a ∼100 fs time scale, with dimer to dimer hopping times very simlar to those within LH1. Furthermore, the B850 depolarization shows a wavelength dependence characteristic of a distribution of pigment site energies within the absorption band. We have utilized the crystallographic information to produce a simple model of the B850 pigments as an excitonically coupled, disordered aggregate. We find that the exciton states are mainly localized on dimeric sites. We propose as a reasonable working model that energy transfer within B850 be regarded as hopping between dimers mediated by a weak-coupling Coulombic mechanism. Electronic structure calculations will be needed in order to clarify the nature of the B850 electronic states and a detailed model required to specify the nature of the optically prepared state. Finally, our data show that excitation transfer from B800 to B850 occurs on the time scale of 650 fs, in agreement with previous room temperature studies.[8,9,16] The structure indicates a pigment separation in which the electronic coupling between donor and acceptor is likely to be dominated by Coulombic interactions (mostly dipolar). However, application of Förster theory with Gaussian approximations to the donor and acceptor spectra yields rates that are 4 orders of magnitude slower than the observed rate. By inclusion of higher lying vibronic states or exciton levels predicted by our model of B850, the calculated time scales fall into the experimentally observed range. We note that the presence of exciton states as possible acceptors is invoked in the case of bacterial reaction centers, in which energy transfer from the accessory bacteriochlorophyll to the special pair occurs in ∼120 fs, which is at least an order of magnitude faster than expected on the basis of weak-coupling Coulombic energy transfer into the lowest exciton state.[42]

Acknowledgment. We thank Frank van Mourik and Rienk van Grondelle for critical readings of the mansucript and Taiha Joo for many useful discussions. R.J. acknowledges the National Physical Science Consortium for a graduate fellowship. This work has been supported by the National Science Foundation.

Appendix

One might question how the ∼45 fs depolarization in the B800 excitation data can be observed when the isotropic rise time of the observed chromophore is ∼650 fs. In order to investigate this point and to contrast the effects of a rise time with the effects of limited time resolution from the IRF, we have fitted simulated data sets: the parallel and perpendicular emission components were calculated from an acceptor (B850) depolarization process with time constants of 100 fs ($r_1 = 0.2$) and 500 fs ($r_2 = 0.1$) which terminates at 0.1. The isotropic rise time is taken to be 50, 200, and 500 fs. The two components are convoluted with the IRF, and Gaussian noise is added. The same signal to noise ratio is used for each data set and is meant to be comparable to that in our experimental data. We use Gaussian IRFs whose widths are 80 and 160 fs fwhm. We subsequently fit the simulated isotropic, parallel, and perpendicular "data" curves with our standard procedures. The results of the fitting are collected in Table 4. For example, in Figure 7 the simulated depolarization data are displayed for a 160 fs IRF and a 500 fs isotropic rise time. In the fit to the

TABLE 4: Fits to Simulated B800−B850 Depolarization

B800−B850 transfer (fs)	IRF (fs)	r_1	τ_1 (fs)	r_2	τ_2 (fs)	r_∞
50	80	0.25	138	0.06	890	0.10
	160	0.22	123	0.07	790	0.10
200	80	0.20	100	0.12	450	0.10
	160	0.09	120	0.17	370	0.10
500	80	0.22	188	0.02	1800	0.10
	160	0.15	86	0.10	430	0.10

anisotropy, we recover time constants of 86 and 430 fs, with an initial value of 0.35. In general, $r(0)$ of the "fitted" anisotropy is usually not 0.4. In most cases, we do not recover precisely the same amplitudes and time constants that were used as input. We find that long rise times have a more pronounced effect on distorting the recovered values than increasing the width of the IRF. The increasing inaccuracy of the recovered depolarization time constants with increasing rise time reflects the signal to noise requirements. Extracting sub-rise time depolarization time constants requires a high signal to noise ratio. Most of the true dynamics will be recovered by the fit if the signal is sufficiently well-averaged.

To examine the effects of B800 to B800 energy transfer in this depolarization, we have simulated the fluorescence depolarization of the B850 subsequent to B800 excitation. The structural and spectral parameters discussed above for B800 monomers and B850 dimers are used to derive the intraband transfer rates. All 9 B800s and 18 B850s are included in the calculation. The transfer rate from B800 to B850 is artificially varied from 110 fs to 2.6 ps, and the results are shown in Figure 8. The simulations reveal two effects. When there is no depolarization among the B800s, the B850 depolarization slows due to "convolution" with the source term (slow B800 to B850 transfer) as compared with direct B850 excitation. The depolarization does not seem to slow further when the B800 to B850 time scale lengthens beyond ∼500 fs. When B800 to B800 transfer is included, the B850 anisotropy decays more quickly than the case where no B800 to B800 transfer takes place. The effects can be summed up as follows: the B850 depolarization reflects the sum of B800 to B800 transfer and B850 to B850 transfer, in combination with a non-exponentiality induced by the B800 to B850 transfer when this rate is slower than the intraband rates. The effects revealed by these simulations show that the fluorescence depolarization of B850 subsequent to B800 excitation does not easily reveal the B800 to B800 energy transfer rate. Resolving B800 to B800 energy transfer with our measurement requires that we accurately determine the time scale of the initial (sub-100 fs) anisotropy decay and compare it to the decay from direct excitation of B850. Due to the subpulse width time scale of this depolarization, we cannot resolve the difference with our present data set.

References and Notes

(1) Van Grondelle, R.; Dekker, J. P.; Gillbro, T.; Sundström, V. *Biochim. Biophys. Acta* **1994**, *1187*, 1−65.
(2) McDermott, G.; Prince, S. M.; Freer, A. A.; Hawthornthwaite-Lawless, A. M.; Papiz, M. Z.; Cogdell, R. J.; Isaacs, N. W. *Nature* **1995**, *374*, 517−521.
(3) Karrasch, S.; Bullough, P. A.; Ghosh, R. *EMBO J.* **1995**, *14*, 631−638.
(4) Kühlbrandt, W. *Nature* **1995**, *374*, 497.
(5) Cogdell, R. J. Private communication.
(6) Fowler, G. J. S.; Visschers, R. W.; Grief, G. G.; van Grondelle, R.; Hunter, C. N. *Nature* **1992**, *355*, 848.
(7) Hess, S.; Visscher, K. J.; Pullerits, T.; Sundström, V.; Fowler, G. J. S.; Hunter, C. N. *Biochemistry* **1995**, *33*, 8300−8305.
(8) Hess. S.; Feldchtein, F.; Babin, A.; Nurgaleev, I.; Pullerits, T.; Sergeev, A.; Sundström, V. *Chem. Phys. Lett.* **1993**, *216*, 247−257.
(9) Shreve, A. P.; Trautmann, J. K.; Frank, H. A.; Owens, T. G.; Albrecht, A. C. *Biochim. Biophys. Acta* **1991**, *1058*, 280−287.
(10) Trautman, J. K.; Shreve, A. P.; Violette, C. A.; Frank, H. A.; Owens, T .G.; Albrecht, A. C. *Proc. Natl. Acad. Sci. USA* **1990**, *87*, 215.
(11) Monshouwer, R.; Ortiz de Zarate, I.; van Mourik, F.; van Grondelle, R. *Chem. Phys. Lett.* **1995**, *246*, 341−346.
(12) Joo, T.; Jia, Y.; Yu, J.; Jonas, D. M.; Fleming, G. R. *J. Phys. Chem.*, in press.
(13) Chachisvilis, M.; Pullerits, T.; Jones, M. R.; Hunter, C. N.; Sundström, V. *Chem. Phys. Lett.* **1994**, *224*, 345−351.
(14) Van Grondelle., R.; Kramer, H. J. M.; Rijgersberg, C. P. *Biochim. Biophys. Acta* **1982**, *682*, 208−215.
(15) Kramer, H. J. M.; van Grondelle., R.; Hunter, C. N.; Westerhuis, W. H. J.; Amesz, J. *Biochim. Biophys. Acta* **1984**, *765*, 156−165.
(16) Bergström, H.; Sundström, V.; van Grondelle, R.; Gillbro, T.; Cogdell, R. J. *Biochim. Biophys. Acta* **1988**, *936*, 90.
(17) De Caro, C.; Visschers, R. W.; van Grondelle, R.; Völker, S. J. *J. Phys. Chem.* **1994**, *98*, 10584−10590.
(18) Reddy, N. R. S.; Small, G. J.; Seibert, M.; Picorel, R. *Chem. Phys. Lett.* **1991**, *181*, 391−399.
(19) Reddy, N. R. S.; Picorel, R.; Small, G. J. *J. Phys. Chem.* **1992**, *96*, 6458−6464.
(20) Warshel, A.; Parson, W. W. *J. Am. Chem. Soc.* **1987**, *109*, 6143−6152.
(21) Renge, I.; Mauring, K.; Avarmaa, R. *J. Lumin.* **1987**, *31*, 207.
(22) Scholes, G. D.; Ghiggino, K. P. *J. Phys. Chem.* **1994**, *98*, 4580−459.
(23) Thompson, M. A.; Zerner, M. C.; Fajer, J. *J. Phys. Chem.* **1991**, *95*, 5693−5700.
(24) Kenkre, V. M. *Phys. Rev. B.* **1978**, *18*, 4064−4076.
(25) Kenkre, V. M.; Reineker, P. In *Exciton Dynamics in Molecular Crystals and Aggregates*; Springer-Verlag: New York, 1982.
(26) Bradforth, S. E.; Jimenez, R.; van Mourik, F.; van Grondelle, R.; Fleming, G. R. *J. Phys. Chem.* **1995**, *99*, 16179−16191.
(27) Jean, J. M.; Fleming, G. R. *J. Chem. Phys.* **1995**, *103*, 2092−2101.
(28) Xie, X.; Du, M.; Mets, L.; Fleming, G. R. *Proceedings of the International Society of Optical Engineers*; SPIE: Bellingham, WA, 1992; p 1640.
(29) Meckenstock, R. U.; Krusche, K.; Staehelin, L. A.; Cyrklaff, M.; Zuber, H. *Biol. Chem. Hoppe-Seyler* **1994**, *375*, 429−438.
(30) Tiede, D. Personal communication.
(31) Cross, A. J.; Fleming. G. R. *Biophys. J.* **1984**, *46*, 45−56.
(32) Chang, J. C. *J. Chem. Phys.* **1977**, *67*, 3901−3909.
(33) Fidder, H.; Knoester, J.; Wiersma, D. A. *J. Chem. Phys.* **1991**, *95*, 7880−7890.
(34) Novoderezhkin, V. I.; Razjivin, A. P. *Biophys. J.* **1995**, *68*, 1089−1100.
(35) Moser, C. C.; Keske, J. M.; Warncke, K.; Farid, R. S.; Dutton, P. L. *Nature* **1992**, *355*, 796−802.
(36) Chang, C. H.; Tiede, D.; Tang, J.; Smith, U.; Norris, J.; Schiffer, M. *FEBS Lett.* **1986**, *205*, 82−86.
(37) Ermler, U.; Fritzsch, G.; Buchanan, S.; Michel, H. *Structure* **1994**, *2*, 925−936.
(38) Förster, Th. In *Modern Quantum Chemistry*; Sinanoglu, O., Ed.; Academic Press: New York, 1965; Vol. III, pp 93−137.
(39) Dexter, D. L. *J. Chem. Phys.* **1953**, *21*, 834−850.
(40) Jean, J.; Chan, C. K.; Fleming, G. R. *Isr. J. Chem.* **1988**, *28*, 169−175.
(41) Jia, Y.; Jonas, D. M.; Joo, T.; Nagasawa, Y.; Lang, M. J.; Fleming, G. R. *J. Phys. Chem.* **1995**, *99*, 6263−6266.
(42) Jonas, D. M.; Lang, M. J.; Nagasawa, Y.; Joo, T.; Fleming, G. R. *J. Phys. Chem.*, submitted.
(43) Magde, D. *J. Chem. Phys.* **1978**, *68*, 3717−3733.
(44) Hess, S.; Åkesson, E.; Cogdell, R. J.; Pullerits, T.; Sundström, V. *Biophys. J.*, in press.
(45) Visschers, R. W.; Chang, M. C.; van Mourik, F.; Parkes-Loach, P. S.; Heller, B. A.; Loach, P. A.; Van Grondelle, R. *Biochemistry* **1991**, *30*, 5734−5742.
(46) Visser, H. M.; Somsen, O. J. G.; van Mourik, F.; Lin, S.; van Stokkum, I. H. M.; Van Grondelle, R. *Biophys. J.* **1995**, *69*, 1083−1099.
(47) Savikhin, S.; Struve, W. S. *Biophys. J.* **1994**, *67*, 2002−2007.
(48) Bradforth, S. E.; Jimenez, R.; Fleming, G. R. Manuscript in preparation.

JP953074J